Analyzing signatures of aerosol-cloud interactions from satellite retrievals and the GISS GCM to constrain the aerosol indirect effect

Surabi Menon,[1] Anthony D. Del Genio,[2,3] Yoram Kaufman,[4] Ralf Bennartz,[5]

Dorothy Koch,[2,3] Norman Loeb,[6] and Daniel Orlikowski[7]

S. Menon, Lawrence Berkeley National Laboratory, 1 Cyclotron Road, MS90KR109, Berkeley, CA 94720, USA. (smenon@lbl.gov)

[1]Lawrence Berkeley National Laboratory,

Abstract.

Evidence of aerosol-cloud interactions are evaluated using satellite data from MODIS, CERES, AMSR-E, reanalysis data from NCEP and data from the NASA Goddard Institute for Space Studies climate model. We evaluate a series of model simulations: (1) Exp N- aerosol direct radiative effects; (2) Exp C- Like Exp N but with aerosol effects on liquid-phase cumulus and stra-

Berkeley, CA, USA

[2]NASA Goddard Institute for Space Studies, New York, NY, USA.

[3]Columbia University, New York, NY, USA.

[4]Formerly at NASA Goddard Space Flight Center, Greenbelt, Maryland, USA, now deceased.

[5]Department of Atmospheric and Oceanic Sciences, University of Wisconsin, Madison, WI, USA

[6]NASA Langley Research Center, Hampton, VI, USA

[7]Lawrence Livermore National Laboratory, Livermore, CA, USA

tus clouds; (3) Exp CN- Like Exp C but with model wind fields nudged to reanalysis data. Comparison between satellite-retrieved data and model simulations for June to August 2002, over the Atlantic Ocean indicate the following: a negative correlation between aerosol optical thickness (AOT) and cloud droplet effective radius (R_{eff}) for all cases and satellite data, except for Exp N; a weak but negative correlation between liquid water path (LWP) and AOT for MODIS and CERES; and a robust increase in cloud cover with AOT for both MODIS and CERES. In all simulations, there is a positive correlation between AOT and both cloud cover and LWP (except in the case of LWP-AOT for Exp CN). The largest slopes are obtained for Exp N, implying that meteorological variability may be an important factor. The main fields associated with AOT variability in NCEP/MODIS data are warmer temperatures and increased subsidence for less clean cases, not well captured by the model. Simulated cloud fields compared with an enhanced data product from MODIS and AMSR-E indicate that model cloud thickness is over-predicted and cloud droplet number is within retrieval uncertainties. Since LWP fields are comparable this implies an under-prediction of R_{eff} and thus an over-prediction of the indirect effect.

1. Introduction

The largest uncertainty in climate forcing from the pre-industrial (PI) time period to the present day (PD) arises from estimates of aerosol-cloud interactions [*Intergovernmental Panel on Climate Change*, 2007]. These aerosol-cloud interactions include the first and second aerosol indirect effects (AIE) [*Twomey*, 1991; *Albrecht*, 1989]. While these effects are often described as a climate forcing, feedbacks associated with the response of cloud properties to changes in the dynamics and the thermodynamic state need to be isolated in order to quantify cloud reflectivity changes due solely to aerosols. Given this ambiguity and the large uncertainty in PD and PI aerosol distributions, predictions of the AIE remain highly uncertain, spanning a range from -0.2 to -4.4 Wm^{-2} [*Menon*, 2004; *Lohmann and Feichter*, 2005].

Satellite observations (such as those from the Moderate Resolution Imaging Spectroradiometer (MODIS)) can potentially decipher cloud responses to aerosol changes [*Kaufman et al.*, 2005a] (hereafter KF05) and thereby constrain model parameterizations of aerosol-cloud interactions [*Lohmann et al.*, 2006; *Quaas and Boucher*, 2005; *Quaas et al.*, 2005; *Chylek et al.*, 2006; *Storelvmo et al.*, 2006]. Such satellite based comparisons [*Lohmann and Lesins*, 2002; *Quaas and Boucher*, 2005] have been used to suggest that the AIE is closer to the smaller magnitude of the range of current predictions (>-1 Wm^{-2}). With observationally-based constraints on PD simulations, predictions of the AIE in future decades appear feasible [*Menon et al.* [2007], in preparation].

With a view to constraining future AIE predictions, we evaluate PD AIE simulations obtained with the NASA Goddard Institute for Space Studies (GISS) global climate model

(ModelE) using satellite data from MODIS and the Clouds and the Earth's Radiant Energy System (CERES). We focus our analyses on the Atlantic Ocean region for the summer season using the same data set from MODIS as analyzed by KF05. KF05 chose the Atlantic since this region is significantly influenced by aerosols of different types at different latitudes: marine aerosols for the 30 to 20S region, biomass aerosols for 20S to 5N, dust for the 5 to 30N region and polluted aerosols for 30 to 60N.

We simulate aerosol effects on liquid-phase cumulus and stratiform clouds and compare to a control simulation that includes only aerosol direct effects. In addition, to test the sensitivity of our results to errors in the GCM general circulation, we conduct another simulation with winds nudged to reanalysis data. Section 2 describes the methodology, satellite data and model simulations; Section 3 compares results from satellite data to model simulations; and in Section 4 reanalysis data from NCEP are examined to evaluate the influence of meteorological errors on cloud properties. Finally in Section 5 we present the summary of our study.

2. Methodology

MODIS-Terra data used in this study are the aggregated 1° daily resolution data for June to August 2002 for the Atlantic Ocean region (30S-60N, 40E -100W) for liquid-phase shallow clouds (cloud top pressure (CTP) >640hPa). Simultaneously retrieved aerosol and cloud properties are available for partly cloud covered 1°x1° areas. We specifically examine aerosol optical thickness (AOT), cloud droplet effective radius (R_{eff}), liquid water path (LWP), water cloud optical thickness (τ_c), cloud cover (CC), cloud top pressure (CTP) and cloud top temperature (CTT). For the GCM, in addition to these we also analyze cloud droplet number concentration (CDNC) and shortwave cloud radiative forcing (SWCRF)

fields. LWP is estimated from the product of R_{eff} and τ_c. An error in MODIS's retrieval procedure that may cause it to report the presence of clouds for large AOT necessitated removal of values for AOT > 0.6 (3% of the data). A similar constraint was also placed on CERES and simulated data. Additionally, meteorological fields from the NCEP reanalysis, namely temperature, horizontal winds and vertical velocity fields at various pressure levels are also examined.

Although MODIS retrievals do not distinguish between types of aerosols, the fractions in the submicron mode allow some distinction between aerosol types as suggested in KF05. Since the contribution of dust aerosols to cloud properties (dependent in part on solubilities assumed and its mixing with other aerosols), is not well known, we estimate the dust contribution to total AOT in the dust zones (5 to 30N) and subtract the dust AOT from the total AOT following *Kaufman et al.* [2005b]. The dust AOT (AOT_{du}) is calculated as:

$$AOT_{du} = \frac{[AOT(f_{an} - f) - AOT_{ma}(f_{an} - f_{ma})]}{(f_{an} - f_{du})} \quad (1)$$

where f, the fine mode fraction is obtained from retrievals and f_{ma}, f_{an}, and f_{du} are the marine, anthropogenic and dust components, respectively, of the fine mode fraction. f is bounded by f_{an} and min[f_{an},f_{du}] and $f_{an} = 0.9\pm0.05$; $f_{du} = 0.5\pm0.05$; $f_{ma} = 0.3\pm0.1$ and $AOT_{ma} = 0.06$. The assumed values for the fine mode fraction for the different aerosol types are obtained from MODIS aerosol measurements in regions with high concentrations of dust, smoke and maritime aerosols. For values of AOT_{du} >0.1 errors are estimated to be upto 10 to 15% as described in *Kaufman et al.* [2005b].

As a check on the MODIS retrieved aerosol and cloud products, particularly R_{eff}, since MODIS retrievals may overestimate R_{eff}, we use data from CERES that include AOT,

R_{eff}, τ_c, LWP and CC. These fields are then compared to data from MODIS as well as model simulated fields. CERES data used here are subject to similar constraints as are MODIS fields for AOT values (AOT<0.6) and we examine liquid-phase low level-clouds (CTP >640hPa) only. The CERES AOT values are determined directly from the MODIS aerosol data product for 10x10 km^2 domains that are simply averaged into CERES footprints by convolving them with the CERES point-spread function. Cloud properties are obtained by applying a cloud retrieval algorithm to MODIS radiances following the methodology of *Minnis et al.* [2003]. These cloud algorithms are different from the ones used to retrieve MODIS cloud properties. While LWP values from both CERES and MODIS are based on the product of R_{eff} and τ_c, R_{eff} for MODIS is based on retrievals from the 2.1 micron channel compared to the 3.7 micron channel used for CERES retrieved R_{eff}. Additionally, for CERES data, a log average value for mean τ_c over a grid box is used compared to a linear average used by MODIS. This essentially results in lower τ_c values for CERES data.

To validate some of the simulated cloud properties, we also use enhanced data-sets described in *Bennartz* [2007] that include CDNC and cloud thickness inferred from MODIS data (onboard Aqua), LWP, τ_c, R_{eff} and CC for assumed adiabatically stratified clouds. The derived LWP product from MODIS is compared to LWP retrievals from the passive microwave Advanced Microwave Scanning Radiometer (AMSR-E) that is co-located with MODIS-Aqua. CDNC and cloud thickness are obtained from independent retrievals of LWP, CC and τ_c along with a few parameters (condensation rate, scattering efficiency and dispersion factor for R_{eff}) that may impact retrieval accuracy depending on the assumptions made. *Bennartz* [2007] estimates a retrieval uncertainty of better than 80%

and 20% for CDNC and cloud thickness, respectively, for cloud fraction >0.8 and higher uncertainties for low LWP and cloud fractions. Furthermore, a difference of a constant factor of 0.83 is expected in LWP estimates based on the vertically homogeneous versus adiabatically stratified cloud assumptions. At low values of LWP, AMSR-E values exceed those from MODIS and at high values the opposite is true. An in-depth explanation of the derivation of the enhanced data products and the retrieval uncertainties are given in *Bennartz* [2007]. The Bennartz products differ from the standard MODIS products we use in several ways: the passage time of Aqua (1:30 pm) is different from that of Terra (10:30 am), adiabatically stratified clouds are assumed as opposed to a vertically homogeneous cloud for the standard MODIS retrievals, and retrievals are only performed by Bennartz for CC > 50%. Thus, we restrict our analysis to a shorter subset of fields: CDNC, R_{eff}, LWP, τ_c and cloud thickness.

For simulations, we use the newly developed GISS GCM (ModelE) [*Schmidt et al.*, 2006] (4°x5° and 20 vertical layers) that includes a microphysics based cumulus scheme [*Del Genio et al.*, 2005], coupled to an on-line aerosol chemistry and transport model [*Koch et al.*, 2007, 2006]. Aerosols simulated include sulfates, organic matter (OM), black carbon (BC) and sea-salt [*Koch et al.*, 2007, 2006], with prescribed dust [*Hansen et al.*, 2005]. A description of the aerosol emissions, processes treated and schemes used to couple the aerosols with the clouds is given in *Koch et al.* [2007] and *Menon and Del Genio* [2007]. PD simulations use emission data from 1995 [*Koch et al.*, 2007], meant to reflect current day conditions. We perform several sets of simulations, mainly to illustrate changes to cloud properties for different representations of aerosol effects on cloud properties.

Table 1 lists the parameterization assumptions used in simulations for CDNC and autoconversion. We calculate R_{eff} as in *Liu and Daum* [2002]:

$$R_{eff} = R_{vol}\beta \tag{2}$$

where R_{vol}, the volume-weighted mean droplet radius is

$$R_{vol} = (\frac{3\mu}{4CDNC\pi\rho_w})^{\frac{1}{3}} \tag{3}$$

and β is an increasing function of the relative dispersion of the cloud drop size distribution (ratio of standard deviation to mean radius) given as

$$\beta = \frac{(1 + 2 * (1 - 0.7 * exp(-0.003 * CDNC))^2)^{\frac{2}{3}}}{(1 + (1 - 0.7 * exp(-0.003 * CDNC))^2)^{\frac{1}{3}}} \tag{4}$$

The τ_c is then calculated as

$$\tau_c = \frac{1.5\mu\Delta H}{R_{eff}\rho_w} \tag{5}$$

Here, μ is the cloud liquid water content (LWC), ρ_w is density of water and ΔH is the cloud thickness.

In simulation Exp N, we do not let aerosols affect cloud microphysics, but we do allow for direct radiative effects of aerosols. In the second simulation, Exp C, we allow aerosols to modify liquid-phase stratus and shallow cumulus clouds, through changes in CDNC and autoconversion as described in Table 1. *Menon and Rotstayn* [2006] performed sensitivity studies with two climate models and found large differences in the AIE and in condensate distributions when including aerosol effects on cumulus clouds. These were related to specific model processes used to distribute cumulus condensate as precipitation or as anvils. Suppression of precipitation in cumulus clouds leads to an increase in detrained condensate especially over ocean regions that in turn increases moisture and condensed

water available for the creation of stratus clouds. Thus, aerosol effects on cumulus clouds indirectly affect LWP and precipitation in stratus clouds. We also perform an additional simulation that mirrors Exp C (Exp CN), except that model horizontal wind fields are nudged to reanalysis data. All runs use climatological mean sea-surface temperatures and are run for 6 years (including a spin up of one year). To compare model fields with satellite retrievals, we use instantaneous values of model fields sampled once every day at cloud top for the last year of the simulation. Model sampling times are chosen to coincide either with data from MODIS on Terra or that from MODIS on Aqua. All data are analyzed for the June to August (JJA) time period.

3. Analysis of aerosol and cloud fields

As in KF05 we examine low-level clouds with average CTP of 866 hPa, between 30S to 60N and 40E to 100W, over oceans. We do not separate the regions based on latitudinal distribution as in KF05, but rather examine differences in fields over the whole domain. Characteristics in AOT and cloud properties from MODIS, CERES and AMSR-E are compared with model simulations as follows:

3.1. Aerosol Optical Thickness

Figure 1 indicates the clear-sky AOT from MODIS, CERES, Exp C and CN. Exp N is comparable to Exp C. The top and middle panels indicate total AOT at 0.55 μm from MODIS and CERES without and with the dust contribution. The bottom panel indicates instantaneous clear-sky total visible AOT without dust from Exp C and CN since we use prescribed dust fields and do not let dust modify cloud properties via its effects on CDNC. If dust contributions are included, higher values of AOT are observed near 5 to 30N (as in

Fig.1 of KF05). A difference in cloud algorithms between MODIS and CERES will lead to sampling differences over regions and days that could cause differences in the AOT values used since the data are sampled for partly-cloudy conditions for simultaneous retrievals of AOT and cloud products. For days and locations that coincide, values are similar for both CERES and MODIS as expected. Major differences between CERES and MODIS AOT are over the dust regions, where differences in total AOT and fine fraction (mainly due to the sampling differences and assumptions used in Eq. (1)) add to produce larger differences in the AOT product filtered for dust. Without the dust filtering, AOT values over the dust zone are fairly similar as shown.

Excluding the larger values of AOT usually found in the dust zones (5 to 30N), the major aerosol regions are off the west coast of Africa (20S to 5N), from biomass source regions, and off the east coast of North America, where the sources are the industrial and transportation sectors. *Kaufman et al.* [2005c] provide an in-depth analysis on MODIS AOT error estimates over the ocean for various issues such as aerosol growth, cloud contamination, sun glint, etc. While cloud contamination causes an error of 0.02 $\pm$0.005 in MODIS AOT, side-scattering from clouds was not found to cause an artificial increase in AOT and is not considered a major issue for analyzing aerosol impacts on cloud microphysics with MODIS [*Kaufman et al.*, 2005c]. A general bias between MODIS AOT and model estimates of AOT of about 0.04 in the mean values for ocean regions is reduced to 0.02 when accounting for aerosol growth [*Kaufman et al.*, 2005c]. The standard error in MODIS AOT over the ocean for non-dust aerosols is δAOT = $\pm$0.05 AOT $\pm$0.03 with slightly higher errors for dust (KF05).

Model estimates of AOT are usually underestimated when compared to observations, especially over tropical oceans [*Kinne et al.*, 2006], and our simulations are no exception. Over the biomass burning areas (west coast of Africa) model AOT is especially underestimated compared to MODIS. With nudged winds, the sea-salt production rate increases since it depends on wind speed, and the overall increase in AOT is about 20%, with increases over most of the domain especially near the biomass zone, due to increased advection of aerosols from the continent (based on wind directions shown in Fig. 7). A previous comparison of model aerosol fields (with similar aerosol effective radii as used in this work but different spatial distributions) with several satellite retrievals indicates that the spatial and seasonal variability are comparable to satellite retrievals, but that the assumed aerosol sizes in the GCM may lead to an underestimation in AOT [*Liu et al.*, 2006]. While assumed aerosol sizes can lead to a factor of two difference in AOT, a deficiency of natural aerosols in southern tropical regions [*Koch et al.*, 2006] can also lead to the lower bias in simulated AOT. However, this should not affect CDNC prediction, that modulates GCM cloud properties, since our CDNC formulation is based on aerosol mass.

3.2. Cloud property changes due to aerosols

In this section we compare model mean cloud property fields with MODIS and CERES. Table 2 indicates mean values and standard deviations of several properties from MODIS, CERES and simulations. While simulated LWP and CC are comparable to MODIS and CERES (except the high/low LWP for Exp N/CERES), simulated AOT values are much lower than MODIS and CERES. Simulated R_{eff} agrees better with CERES than MODIS. Reasons for the differences in these products are discussed as follows:

3.2.1. Variation in cloud droplet size and liquid water path with AOT

Figure 2 shows the R_{eff} distributions from MODIS, CERES and Exp C, as well as the simulated CDNC from Exp C. Although model AOT is underestimated, there is clear evidence of a change (larger values) in CDNC (dependent on mass-based estimates of aerosols) between the North and South Atlantic, and to some extent along the continental edges, where R_{eff} is also smaller, somewhat similar to the changes evident in MODIS AOT retrievals. In general, model cloud fields exhibit smaller R_{eff} and larger CDNC (except for Exp N since CDNC is constant) in the more polluted North Atlantic sector (sulfate and carbonaceous aerosols from fossil- and biofuel are more dominant in the North Atlantic and sea-salt and carbonaceous aerosols from biomass are more prevalent in the South Atlantic).

Simulated R_{eff} is largely underestimated compared to that retrieved from MODIS, and around 1 μm smaller compared to CERES, as shown in Table 2 and Fig. 2. Similar results for comparison of model simulated R_{eff} fields with MODIS were obtained from other studies [*Storelvmo et al.*, 2006; *Lohmann et al.*, 2006]. For bumpy inhomogeneous cloud fields MODIS may over-predict R_{eff} and under-predict τ_c, though this should not preclude using the dataset to examine changes in R_{eff} for changing AOT conditions (KF05). Values retrieved from CERES are much lower than MODIS, especially along the eastern parts of the Atlantic. Differences in retrievals from the 2.1 versus 3.7 micron channel used for MODIS and CERES, respectively, alone cannot account for the differences in retrieved R_{eff} and exact reasons for the differences are not known and is beyond the scope of this analysis.

In general, R_{eff} in Fig. 2 is smaller in polluted regions than in cleaner regions in both datasets and in Exp C and CN. The same is not true for Exp N (not shown). By definition

of the first AIE, an increase in AOT can lead to a decrease in R_{eff} if LWC stays unchanged. LWC estimates are not available from satellite, but the spatial relationships we observe are at least consistent with an AIE signal. Since model differences in R_{eff} for increases in AOT for Exp C and Exp CN are smaller than those from MODIS and CERES, we analyze the variability between AOT and R_{eff} for different ranges of LWP, since varying LWP may influence the R_{eff}-AOT relationship. Figure 3 shows the correlation coefficients for R_{eff}-AOT versus LWP averaged over selected LWP bins (20 gm^{-2} for LWP <100 gm^{-2}; 50 gm^{-2} for 100 < LWP < 350 gm^{-2}; and for LWP > 350 gm^{-2}) for CERES, MODIS, and Exp N, C and CN. For cases where LWP values are roughly similar, the negative correlations between R_{eff} and AOT should prevail if aerosols influence R_{eff}. As shown in Fig. 3, both MODIS and CERES indicate a negative correlation between R_{eff} and AOT, except at the higher ranges in LWP where CERES indicates a positive correlation for R_{eff}-AOT. For simulations, Exp C is mostly negative, whereas Exp CN and Exp N are more positive. For Exp N, since LWP values are rather large and CDNC is fixed, R_{eff} also increases since we have no aerosol-induced modification of cloud properties (autocoversion is a function of condensate only) that may alter the distribution of LWP that may be more determined by non aerosol-cloud effects.

Thus, the positive correlations we find cannot simply be explained as that due to varying LWP. Modifications to the precipitation efficiency may result in situations where LWP may increase or decrease with increasing aerosols. This was found to depend on the humidity conditions above cloud and the entrainment of dry air, such that only for moist overlying air masses with low CDNC does cloud water increase with aerosols; and for cases with enhanced entrainment of dry air, cloud water decreases with an increase in CDNC

[*Ackerman et al.*, 2005]. Spatial distributions of the correlation between LWP and AOT for MODIS, CERES and simulations indicate an overall positive relationship with a negative correlation found in biomass regions and the eastern North Atlantic region for MODIS and to some extent for CERES. The increase in LWP with AOT is more pronounced in Exp N, indicating that non aerosol-cloud effects play a stronger role in modulating LWP over the ocean. Since LWP is a derived product and may mask liquid water variability if cloud thickness varies, a more conclusive reasoning for spatial variations between R_{eff} with AOT is hard to obtain.

Thus, observational signals to evaluate the first and second AIE are complicated, since these include changes to LWP and CC that may even be more obscured by feedbacks or meteorological variability. As shown in Table 2, mean LWP fields for Exp C and CN are somewhat comparable to MODIS (about 5% higher), but are higher than CERES. The lower LWP values for CERES compared to MODIS may partly be related to the log average values used for τ_c and the lower R_{eff}. However, since LWP is a derived product for both CERES and MODIS, evaluation of this field may be obscured if there are biases in τ_c and R_{eff}. Since we cannot evaluate retrieval uncertainties in these products within the scope of our analysis, to at least understand if biases exist in simulated R_{eff} and τ_c, the standard (τ_c, R_{eff}) and enhanced data products, such as CDNC and cloud thickness, derived from MODIS (on Aqua) with collocated retrievals of LWP from AMSR-E from *Bennartz* [2007] are used to evaluate some of the cloud microphysics products from Exp C.

3.2.2. Simulated cloud microphysical fields versus those derived from satellite

Here, we perform an analysis of cloud microphysical fields using the derived data set from *Bennartz* [2007] that includes cloud thickness, CDNC, τ_c, R_{eff} and LWP from MODIS (onboard Aqua) versus those simulated for Exp C. Also included are LWP retrievals from AMSR-E (also onboard Aqua). These data sets (both for retrievals and simulations) are obtained at a different time interval than those used in the prior sections and do not include AOT fields. Figure 4 shows CDNC, cloud thickness, R_{eff} and τ_c inferred from MODIS and that from Exp C. Figure 5 shows LWP inferred from MODIS, obtained from AMSR-E and that from Exp C. In general, we note that model CDNC values are within retrieval uncertainties (though lower by 46% compared to the average value inferred from MODIS) and cloud thickness is over-predicted by a factor of 1.5 compared to the average values obtained from retrievals. The apparent differences in CDNC fields may in part be related to assumptions used in CDNC calculations for simulations, that are based on empirical observations and do not capture the higher values, especially near continental edges, and the higher uncertainty in CDNC estimates from retrievals (80%), especially at low LWP values found here (see for example Fig. 3 in *Bennartz* [2007]).

LWP values for Exp C (average of 76 gm^{-2}) are comparable to MODIS and AMSR-E (70 gm^{-2}), thus suggesting that liquid water contents in the model may be under-estimated since LWP is the vertical integral of LWC over cloud thickness. However, since the uncertainty in cloud thickness retrievals are small (20%) and models in general tend to over predict cloud thickness (coarse resolution being one aspect of the problem since all simulations have similar cloud thickness values), the over-prediction of simulated cloud thickness must imply lower LWC values for simulations that include aerosol-induced cloud modifications.

Estimates for R_{eff} for Exp C (average of 12.2 μm) are about 2 μm smaller than that retrieved for MODIS (14.3 μm) and τ_c values for Exp C (9.2) were comparable to MODIS (8.6). Closer agreement between MODIS and Exp C indicated here, compared to values shown in Table 2, may be related to the uncertainties in the simulated diurnal cycle of the clouds or retrieval issues that are more difficult to verify. Retrieval assumptions for vertically homogeneous versus adiabatically stratified clouds should not lead to differences in R_{eff} and τ_c retrievals nor should differences in the dispersion term used to convert r_{vol} to R_{eff} for MODIS and Exp C (an average value of 1.08 $\pm$0.06 is used by *Bennartz* [2007], and for Exp C the value for dispersion (given by the β term in Eq. 1) varies between 1.1 and 1.6 with a central value of 1.14$\pm$0.05). Based on the above comparisons we find that simulated CDNC is within retrieval uncertainties but low biases exist in simulated cloud liquid water (based on the over-estimation of cloud thickness) and thus, R_{eff}.

3.2.3. Estimating the response of cloud property changes to AOT

Patterns of correlations between all the variables examined here (from MODIS-Terra, CERES and simulations) with AOT are shown in Fig. 6 and provide a visual analysis of trends across simulations, MODIS and CERES (CERES values for CTT are not available here and are indicated as 0). MODIS does indicate an increase in CC and τ_c and a decrease in R_{eff} with increasing AOT as does CERES. Other variables, such as CTT and CTP appear to be more correlated to CC (negative correlations) than AOT, with a somewhat positive association between warmer clouds and AOT and a negative correlation between CTP and AOT. However, CERES indicates a positive relationship between CTP and AOT similar to simulations. In all simulations, an overall increase in LWP (except for Exp CN), τ_c and CC with aerosols is observed, especially for Exp N.

Since the relationships between cloud properties and aerosols are not necessarily linear, we examine the magnitudes of slopes based on log-log [*Sekiguchi et al.*, 2003] or log-linear relationships, depending on the range and best fit line to the data. Table 3 shows the slopes between AOT and the variables of interest for MODIS, CERES and simulations. We note that model slopes for R_{eff} and AOT are severely underestimated w.r.t. MODIS and CERES. Only Exp N (without aerosol-induced changes to cloud microphysics) exhibits a positive correlation between AOT and R_{eff} (due to the higher LWP and fixed CDNC). For LWP versus AOT, the positive slopes for Exp N and Exp C are in contrast to the negative slopes from MODIS, CERES and Exp CN. However, only the slopes for Exp N and CERES were significant at the 95% level. The larger slope for Exp N indicates that meteorological effects play a role in increasing LWP in areas with high AOT.

For CC versus AOT, slopes from all simulations are positive, similar to MODIS and CERES, but a few factors lower. Since all simulations had fairly similar slopes, we note that meteorological variability or non-aerosol-cloud effects appear to explain most of the increase in CC with AOT, similar to the results in *Lohmann et al.* [2006] that indicate a more dominant non aerosol-cloud effect on CC increase with AOT. As CC increases, so does relative humidity in the clear regions adjacent to the clouds, resulting in an increase in AOT and an apparent correlation between AOT and CC. Recent 3D Monte Carlo simulations of side-scattering from clouds qualitatively capture both increases in AOT with CC and the spectral dependence in AOT with CC seen in the satellite retrievals [*Wen et al.*, 2007]. This may explain some of the larger slopes seen in MODIS and perhaps CERES. Additionally, changes in CC and AOT over regions subject to different dynamical forcings and different aerosol sources may cause an apparent correlation between AOT and

CC that may be misinterpreted as aerosol-cloud interactions. Thus, based on simulations and the uncertainty in retrievals, correlated changes in CC and aerosols may in large part be related to meteorological and aerosol humidification effects.

Comparing τ_c-AOT slopes between model and MODIS/CERES indicates that model values for Exp N and Exp C are higher than MODIS and CERES, primarily due to the lower AOT and the higher τ_c and the variability in LWP. To understand the changes in radiative fields, we compare the slopes of SWCRF-AOT amongst simulations. CERES derived values for SWCRF were not directly comparable to simulated values and hence is not compared to simulations. For SWCRF versus AOT, Exp C is of similar magnitude but of opposite sign compared to Exp N. Exp CN is a factor of 1.5 greater than Exp C. Thus, changes in the radiative fields (SWCRF) from aerosol-induced changes to cloud microphysics are a factor of 2 to 3 higher than that obtained from non aerosol-cloud effects. Interestingly, *Lohmann et al.* [2006] find that aerosol-induced changes to cloud microphysics account for 25% of the change in SWCRF, for simulations with and without aerosol-cloud interactions. Using τ_c-AOT and CC-AOT slope differences between Exp N and Exp C, we estimate that non aerosol-cloud effects accounts for 57% of the increase in τ_c simulated by Exp C and completely dominate the CC increase.

Though the mean values for the various properties are similar in Exp C and Exp CN (except for SWCRF), as shown in Table 2, overall the magnitude of the slopes for Exp CN are in slightly better agreement with MODIS and CERES than are the slopes for Exp C (as shown in Table 3). Thus, nudging to observed wind fields with aerosol induced modification to cloud properties creates conditions that are in closer agreement to satellite-based retrievals. Clearly, wind-fields and their effects on the response of R_{eff}, LWP and

thus τ_c and SWCRF to AOT are different that may be due to AOT fields themselves that increase slightly with nudged winds, probably resulting in more aerosols advected from the continent.

Thus, in general, model slopes for R_{eff} and CC are underestimated compared to MODIS and CERES and the τ_c-AOT slope is generally overestimated (probably due to the underprediction of R_{eff} as noted in Sec.3.2.2, and AOT). The largest uncertainty in such an inference relates to the LWC and meteorological variability with AOT.

4. Meteorological influence on aerosol and cloud properties

To further explore the influence of meteorology on cloud properties, we evaluate temperature, wind and vertical velocity fields from NCEP and model simulations. Figure 7 shows temperature and wind fields from NCEP and Exp C at 1000 hPa. Mean temperature fields (at 1000 hPa) from NCEP indicate higher values in the northern tropics along the east coast of S. America and higher values at 750 hPa along the dust (10-30N) and biomass (10-20S) zones. NCEP wind fields indicate the presence of easterly winds between 0 to 15N and south-easterly winds from 20S to 0, transporting dust and biomass layers towards S America. For the N. Atlantic sector, between 40 to 60N, air masses (perhaps polluted) from N. America are transported towards Europe. The simulations do capture the spatial distribution of the temperature fields, with higher values over the tropical areas compared to NCEP. The prevailing wind fields are also comparable to NCEP, except for weaker westerlies in the N. Atlantic sector. The wind field strength increases in simulations with aerosol-cloud interactions (especially for the nudged case) compared to Exp N.

NCEP vertical velocity fields indicate uniformally low subsidence over most of the domain at 750 hPa (and a bit more so at 500 hPa) except near the equator, where ascent is observed. Figure 8 shows the probability density function for geometric vertical velocity at 750 hPa (positive upward) from NCEP and from the simulations. Simulated subsidence rates are weaker for all model simulations than for NCEP; nudging of winds has only a minimal effect.

To understand changes to aerosol and clouds fields due to meteorological influences, KF05 performed multiple regression analyses to judge the relative influence of the various fields and found temperature, followed by wind fields to be more important. We perform similar analysis, using NCEP and model fields, but instead characterize differences based on the probability density distributions for particular AOT conditions (above or below the baseline value of 0.06 for AOT). Figure 9 shows the probability density distributions for temperature, the U and V component of the horizontal wind fields at 1000 hPa and vertical velocity fields at 750 hPa, for AOT values below and above 0.06 for MODIS and the three simulations. Results were similar at other levels (750 and 500 hPa), unless noted otherwise. Results from Fig.9 indicate an increase in warmer conditions for higher values of AOT (>0.06). This may be simply related to location of aerosol source regions (e.g. higher dust and biomass sources near the tropics). For simulations, only a slight tendency towards higher temperature was obtained for differences in AOT. For the high AOT cases, the mean temperature from NCEP and simulations were similar, but for the low AOT cases, the mean temperature was about 2 degrees warmer for simulations compared to NCEP. For wind fields, for low (AOT<0.06) and high AOT cases, NCEP indicates a slight tendency for easterly and southerly components for the higher AOT cases, and the

simulations (especially Exp CN) follow the NCEP distribution for the low AOT case but the southerly component for the high AOT case is not well simulated.

Vertical velocity fields for both NCEP and simulations are similar and exhibit no significant changes for differences in AOT values. To investigate the association of cloudiness and pollution with regions of subsidence that could lower the PBL height and trap pollution, we further separate the vertical velocity fields to areas of negative velocities only. We find no strong evidence of increased subsidence strength associated with clean or less clean cases from simulations. However, NCEP data do indicate a factor of 2 increase in subsidence strength for the less clean compared to the clean cases. In subsidence regions CC does increase for MODIS (62%) and all simulations (about 9%) for the less clean cases. The increase is similar to that found for all conditions (positive and negative vertical velocity regions). Further analysis of CC changes in areas of greater subsidence (subsidence values greater than the mean) do not indicate any significant changes in CC based on changes in subsidence strengths.

5. Summary

To evaluate model predictions of the aerosol indirect effect, we compare a series of model simulations with and without aerosol effects on cloud microphysics with data from MODIS, CERES, AMSR-E and NCEP for the Atlantic Ocean region for June to August 2002. Cloud response to aerosols for liquid-phase shallow clouds are studied in the different simulations that include the aerosol direct effect (Exp N), aerosol effects on stratus and cumulus clouds (Exp C), and for a simulation that mirrors Exp C but with model horizontal winds nudged to reanalysis data (Exp CN). Analysis of model simulations using correlation matrices and slopes indicate that simulations without aerosol-induced changes

to cloud microphysics (Exp N) did not capture the reduction in R_{eff} with increasing AOT seen in satellite data since the less clean cases have a large increase in the LWP fields, from meteorological effects that dominates the changes in R_{eff}, and CDNC is fixed in these simulations. For Exp N, LWP was positively correlated to AOT in contrast to the negative relationship found for MODIS (not significant) and CERES. The correlation between LWP and AOT for Exp C (positive) and Exp CN (negative) were not significant. While both MODIS and CERES data did indicate a strong increase in CC with AOT, all simulations capture a similar increase, though of lesser magnitude, with non aerosol-cloud effects dominating CC changes. Although features in Exp CN are also present in Exp C, nudging to wind fields results in simulations with different dynamics and these simulations improve the response of cloud properties to AOT (based on the comparison of slopes obtained for simulations versus that for CERES and MODIS shown in Table 3). This appears to be due to slightly higher values of AOT in Exp CN (nudging to wind fields helps advect more aerosols from the continent to the ocean thereby reducing the generally low model AOT bias). However, based on the signs of the slopes, these changes are smaller than are changes associated with not including aerosol-induced cloud modifications.

An association between warmer temperature and higher AOT was found for NCEP and to a somewhat weaker extent in all simulations. We find a slight increase in the easterly and southerly wind fields with an increase in AOT (more so for NCEP than the GCM) and no association between vertical velocities and AOT. While there was no association between subsidence strength and pollution for the simulations, NCEP/MODIS did indicate an increase in subsidence strength (factor of 2) for the less clean versus the clean case. An increase in CC with aerosols in areas of subsidence was found for both

NCEP/MODIS fields and simulations that was of similar strength as that obtained for cases without separating the data into subsidence only regions, indicating that aerosols were more influential than large-scale subsidence in changing CC.

Comparing the magnitudes of the slopes between R_{eff}-AOT for MODIS/CERES and Exp C, as a measure of the relative changes in cloud properties due to aerosols, we note that model slopes are underestimated. However, the τ_c-AOT slope is overestimated by the model (except for Exp CN) compared to MODIS and CERES, and this relates to the variability and slope of the LWP-AOT relationship that was different between MODIS, CERES and the simulations, especially Exp N. Clearly, the variability in LWP and an independent accurate measure of liquid water are critical to AIE estimates.

Constraining cloud properties (cloud thickness and CDNC) simulated by Exp C with those inferred from the enhanced MODIS data set used here (onboard Aqua) and based on estimates of co-located LWP fields (MODIS and AMSR-E), we conclude that the model CDNC fields are within retrieval uncertainties but the model significantly over-predicts cloud thickness (factor of 1.5). Since simulated LWP values are comparable to satellite estimates, this could imply that simulated LWC and R_{eff} are also under-predicted. Cloud changes –increase with an increase in aerosols– are quite robust in MODIS and CERES data. While cloud changes with aerosols were not as strong in simulations, similar values found for all simulations suggest that meteorological variability may play a stronger role in modulating CC. τ_c-AOT and CC-AOT slope differences between Exp C and Exp N indicate that meteorological variability accounts for a 57% increase in τ_c and dominates the CC increase. We estimate changes in the SWCRF fields from aerosol-induced modifications to cloud properties are a factor of 2-3 greater than without aerosol-induced

changes to cloud properties, based on the estimated slopes between SWCRF and AOT for the three simulations (Exp N, C and CN), due to the stronger first AIE.

For Exp C, we obtain an annual global average AIE value (defined as the difference in net cloud radiative forcing between Year 2030 –for the IPCC midline A1B scenario described in *Unger et al.* [2006]– and Year 2000) of -0.68 W m^{-2} [*Menon et al.*, 2007]. The average value for June to August for the Atlantic Ocean region studied here is -0.50 Wm^{-2}. Using the best-guess estimate from retrievals (R_{eff} from CERES, τ_c from MODIS and CC from both), we attempt to evaluate if our AIE is over or under- predicted for Exp C, based on changes in τ_c, R_{eff} and CC with AOT. From Table 3, we find that:
(1) the slope of CC w.r.t. AOT is underestimated by ∼80% and 70%, compared to MODIS and CERES, respectively;
(2) the slope of τ_c w.r.t. AOT is about a factor of 2.2 higher compared to MODIS; and
(3) the slope of R_{eff} w.r.t AOT is underestimated by 90% compared to CERES.
Thus, as a rough approximation we estimate that Exp C may slightly over-predict the indirect effect compared to best-guess MODIS/CERES estimates.

Summarizing the main points of our study, in spite of several caveats present in satellite and model fields analyzed here, we find that:
(1)R_{eff} decreases with an increase in AOT, averaged over the entire domain, are robust in MODIS and CERES retrievals and are present to some extent in simulations where aerosols modify cloud properties;
(2)CC increases with AOT are especially robust in MODIS and CERES retrievals and are also noted in model simulations, with meteorological variability providing the dominant signal for simulated CC changes;

(3)τ_c increases with an increase in AOT in MODIS and CERES are smaller compared to simulations;

(4) association between a small subset of large-scale meteorological fields examined here (temperature, horizontal winds and vertical velocity) and AOT, from NCEP and simulations indicate warmer temperatures in areas of higher AOT (>0.06), more related to location of source regions, and an increase in subsidence strength with pollution for NCEP/MODIS;

(5) nudging to wind fields in simulations that include aerosol-induced changes to clouds improves the response of cloud properties to differences in AOT (based on slopes between Exp C, CN, MODIS and CERES shown in Table 3) probably due to improved AOT distributions themselves;

(6) our standard simulation (Exp C) predicts CDNC within retrieval uncertainties but under-predicts LWC compared to data inferred from MODIS and AMSR-E and thus may under-predict R_{eff}; that may explain the overestimation in τ_c and SWCRF.

We believe that the above analyses can only be considered as a very broad approximation or a first guess attempt to constrain the AIE magnitude. Contextualizing the major objective of this work, constraining present-day AIE simulations to better predict the future, it appears that our values for Exp C, our standard simulation, may only be slightly overestimated for the ocean region. To better understand the global-scale implications of the above analysis since land signals are different compared to ocean signals (AOT and CDNC values and thus AIE are higher over land), ongoing future work will extend the present analysis globally with an emphasis on variations of key features of aerosol-cloud

interactions isolated for specific meteorological regimes with co-located MODIS, AMSR-E and radiation data from CERES.

Acknowledgments. We gratefully acknowledge funding from the NASA MAP and Radiation Sciences Program managed by Don Anderson and Tsengdar Lee. This paper is dedicated to the memory of Yoram Kaufman. We gratefully acknowledge the contributions from S. Bauer, whose reanalyses techniques have been used in model simulations, and I. Koren and S. Mattoo for help with interpreting MODIS and NCEP data used in this study.

References

Ackerman, A. S., M. P. Kirkpatrick, D. E. Stevens, and O. B. Toon, The impact of humidity above stratiform clouds on indirect aerosol climate forcing, *Nature*, *432*, 1014–1017, 2005.

Albrecht, B. A., Aerosols, cloud microphysics, and fractional cloudiness, *Science*, *245*, 1227–1230, 1989.

Bennartz, R., Global assessment of marine boundary layer cloud droplet number concentration from satellite, *J. Geophys. Res.*, *112*, doi:10.1029/2006JD007547, 2007.

Chylek, P., M. Dubey, U. Lohmann, V. Ramanathan, Y. Kaufmann, G. Lesins, J. Hudson, G. Altmann, and S. Olsen, Aerosol indirect effect over the Indian Ocean, *Geophys. Res. Lett.*, *33*, L06,806, 2006.

Del Genio, A. D., M.-S. Yao, W. Kovari, and K.-W. Lo, A prognostic cloud water parameterization for global climate models, *J. Climate*, *9*, 270–304, 1996.

Del Genio, A. D., W. Kovari, M.-S. Yao, and J. Jonas, Cumulus microphhysics and climate sensitivity, *J. Climate*, *18*, 2376–2387, 2005.

Hansen, J., M. Sato, R. Ruedy, L. Nazarenko, and A. L. et al., Efficacy of climate forcings, *J. Geophys. Res.*, *110*, doi:101029/2005JD005776, 2005.

Intergovernmental Panel on Climate Change, *Climate Change 2007: The Physical Science Basis*, Cambridge University Press, (S. Solomon, D. Qin, M. Manning, Z. Chen, M. Marquis, K.B. Averyt, M.Tignor and H.L. Miller , Eds.), 2007.

Kaufman, Y., I. Koren, L. Remer, D. Rosenfeld, and Y. Rudich, The effect of smoke, dust, and pollution aerosol on shallow cloud development over the Atlantic Ocean, *Proc. Natl. Acad. Sci.*, *32*, 11,207–11,212, 2005a.

Kaufman, Y., I. Koren, L. Remer, D. Tanre, P. Ginoux, and S. Fan, Dust transport and deposition observed from the Terra-Moderate Resolution Imaging Spectroradiometer (MODIS) spacecraft over the Atlantic Ocean, *J. Geophys. Res.*, *100*, doi:10.1029/2003JD004436, 2005b.

Kaufman, Y., et al., A critical examination of the residual cloud contamination and diurnal sampling effects on modis estimates of aerosol over ocean, *IEEE Trans. Geosci. Remote Sens.*, *43*, 2886–2897, 2005c.

Kinne, S., M. Schulz, C. Textor, S. Guibert, and U. L. et al., An aerocom initial assessment - optical properties in aerosol component modules of global models, *Atmos. Chem. Phys. Discuss.*, *6*, 1815–1834, 2006.

Koch, D., G. Schmidt, and C. Field, Sulfur, sea salt and radionuclide aerosols in GISS, ModelE, *J. Geophys. Res.*, *111*, d06206,doi:10.1029/2004JD005550, 2006.

565 Koch, D., T. Bond, D. Streets, N. Unger, and G. van der Werf, Global impacts
566 of aerosols from particular source regions and sectors, *J. Geophys. Res.*, *111*,
567 d02205,doi:10.1029/2005JD007024, 2007.

568 Liu, L., A. Lacis, B. Carlson, M. Mishchenko, and B. Cairns, Assessing a GCM aerosol
569 climatology using satellite and ground-based measurements: A comparison study, *J.*
570 *Geophys. Res.*, *111*, doi:10.1029/2006JD007334, 2006.

571 Liu, Y., and P. Daum, Anthropogenic aerosols: Indirect warming effect from dispersion
572 forcing, *Nature*, *419*, 580–581, 2002.

573 Lohmann, U., and J. Feichter, Global indirect aerosol effects: A review, *Atmos. Chem.*
574 *Phys. Discuss.*, *5*, 715–737, 2005.

575 Lohmann, U., and G. Lesins, Stronger constraints on the anthropogenic indirect aerosol
576 effect, *Science*, *298*, 1012–1016, 2002.

577 Lohmann, U., I. Koren, and Y. Kaufman, Disentangling the role of microphysical and
578 dynamical effects in determining cloud properties over the Atlantic, *Geophys. Res. Lett.*,
579 *33*, L09,802, 2006.

580 Menon, S., Current uncertainties in assessing aerosol effects on climate, *Ann. Rev. Envi-*
581 *ron. Resour.*, *29*, 1–30, 2004.

582 Menon, S., and A. Del Genio, *Evaluating the impacts of carbonaceous aerosols on clouds*
583 *and climate. In Human-induced climate change:An interdisciplinary assessment*, Cam-
584 bridge University Press, (M. Schlesinger et al., Eds.), 2007.

585 Menon, S., and L. Rotstayn, The radiative influence of aerosol effects on liquid-phase
586 cumulus and stratus clouds based on sensitivity studies with two climate models, *Clim.*
587 *Dyn.*, *27*, 345–356, 2006.

588 Menon, S., N. Unger, D. Koch, D. Streets, D. Shindell, A. Del Genio, and J. Hansen,
589 Aerosol-cloud interactions and climate change for 1980-2030, *Env. Res. Lettr.*, to be
590 submitted, 2007.

591 Minnis, P., D. F. Young, S. Sun-Mack, P. W. Heck, D. R. Doelling, and Q. Trepte, CERES
592 cloud property retrievals from imagers on TRMM, Terra, and Aqua, *Proc. SPIE 10th*
593 *Int. Symp. on Remote Sensing: Conf. on Remote Sensing of Clouds and the Atmosphere*
594 *VII, Barcelona, Spain*, pp. 37–48, 2003.

595 Quaas, J., and O. Boucher, Constraining the first aerosol indirect radiative forcing in
596 the LMDZ GCM using POLDER and MODIS satellite data, *Geophys. Res. Lett.*, *32*,
597 L17,814, 2005.

598 Quaas, J., O. Boucher, and U. Lohmann, Constraining the total aerosol indirect effect
599 in the LMDZ and ECHAM4 GCMs using MODIS satellite data, *Atmos. Chem. Phys.*
600 *Discuss.*, *5*, 9669–9690, 2005.

601 Rotstayn, L. D., and Y. Liu, A smaller global estimate of the second indirect aerosol
602 effect, *Geophys. Res. Lett.*, *32*, doi:10.1029/GL021922, 2005.

603 Schmidt, G. A., R. Ruedy, J. E. Hansen, I. Aleinov, and N. B. et al., Present day atmo-
604 spheric simulations using GISS ModelE: comparison to in-situ, satellite and reanalysis
605 data, *J. Climate*, *19*, 153–192, 2006.

606 Sekiguchi, M., T. Nakajima, K. Suzuki, K. kawamoto, A. Higurashi, D. Rosenfeld,
607 I. Sano, and S. Mukai, A study of the direct and indirect effects of aerosols us-
608 ing global satellite data sets of aerosol and cloud parameters, *J. Geophys. Res.*, *108*,
609 doi:10.1029/2002JD003359, 2003.

Storelvmo, T., J. Kristjansson, G. Myhre, M. Johnsrud, and F. Stordal, Combined observational and modeling based study of the aerosol indirect effect, *Atmos. Chem. Phys. Discuss.*, *6*, 3757–3799, 2006.

Twomey, S., Aerosols, clouds and radiation, *Atmos. Environ.*, *25*, 2435–2442, 1991.

Unger, N., D. Shindell, D. Koch, and D. Streets, Cross influences of ozone and sulfate precursor emissions changes on air quality and climate, *Proc. Natl. Acad. Sci.*, *103*, 4377–4380, 2006.

Wen, G., A. Marshak, R. Cahalan, L. Remer, and R. Kleidmand, 3d aerosol-cloud radiative interaction observed in collocated MODIS and ASTER images of cumulus cloud fields, *J. Geophys. Res.*, in Review, 2007.

Table 1. Expressions used to obtain the cloud droplet number concentration (CDNC) and autoconversion for simulations. N_a is the aerosol concentration obtained from the aerosol mass for a log-normal distribution as described in *Menon and Rotstayn* [2006].

Variable	Exp N	Exp C-Stratus	Exp C-Cumulus
CDNC-land	175	-598+298 $\log(N_a)$	174.8 + 1.51 $N_a^{0.886}$
CDNC-ocean	60	-273+162 $\log(N_a)$	-29.6+4.92$N_a^{0.694}$
Autoconversion	f(condensate) [*Del Genio et al.*, 1996]	f(droplet threshold size) [*Rotstayn and Liu*, 2005]	f(droplet threshold size) [*Menon and Rotstayn*, 2006]

Table 2. Average and standard deviations for aerosol optical thickness (AOT), cloud droplet effective radii (R_{eff}) (μm), liquid water path (LWP) (gm^{-2}), cloud cover (CC) (%), cloud optical depth (τ_c), cloud top temperature (CTT) (K) and cloud top pressure (CTP) (hPa) for MODIS, CERES and the three simulations. Also included for model simulations are shortwave cloud radiative forcing (SWCRF) (Wm^{-2}) values.

Values	MODIS	CERES	Exp N	Exp C	Exp CN
AOT	0.13±0.09	0.13±0.11	0.06±0.05	0.06±0.05	0.07±0.05
R_{eff}	16.7±4.70	13.7±4.36	13.1±4.22	12.6±3.34	12.3±4.02
LWP	67.4±46.7	43.8±37.6	134±167	71.9±65.2	70.6±68.8
CC	41.0±31.6	54.1±32.3	44.9±19.8	46.5±19.3	45.7±20.0
τ_c	5.82±3.52	3.10±3.00	12.8±9.79	8.77±9.17	8.96±10.1
CTT	288±3.62	NA	289±5.38	289±5.33	290±5.41
CTP	866±67.7	878±50.9	896±54.9	895±58.2	898±56.9
SWCRF	NA	NA	-101 ±134	-103±129	-89.9±120

Table 3. Summary of slopes between cloud droplet effective radii (R_{eff}), liquid water path (LWP), cloud cover (CC), cloud optical depth (τ_c) and shortwave cloud radiative forcing (SWCRF) versus aerosol optical thickness (AOT) for log-log (1) and log-linear (2) relationships for MODIS, CERES and model simulations. Values that are not significant ($p<0.05$) based on the Student's t-test are indicated in italics.

Slope	MODIS	CERES	Exp N	Exp C	Exp CN
R_{eff}-AOT (1)	-0.11 ±0.001	-0.17±0.001	0.06±0.01	-0.02±0.008	-0.06±0.01
LWP-AOT (1)	*-0.004±0.003*	-0.07±0.03	0.09±0.04	*0.005±0.03*	*-0.04±0.04*
CC-AOT (1)	0.40±0.005	0.23±0.004	0.07±0.01	0.07±0.01	0.05±0.02
τ_c-AOT (2)	0.61±0.01	0.75±0.01	1.12±0.24	1.95±0.22	0.60±0.28
SWCRF-AOT (2)	NA	NA	15.2±3.27	-13.0±3.09	-33.1±3.29

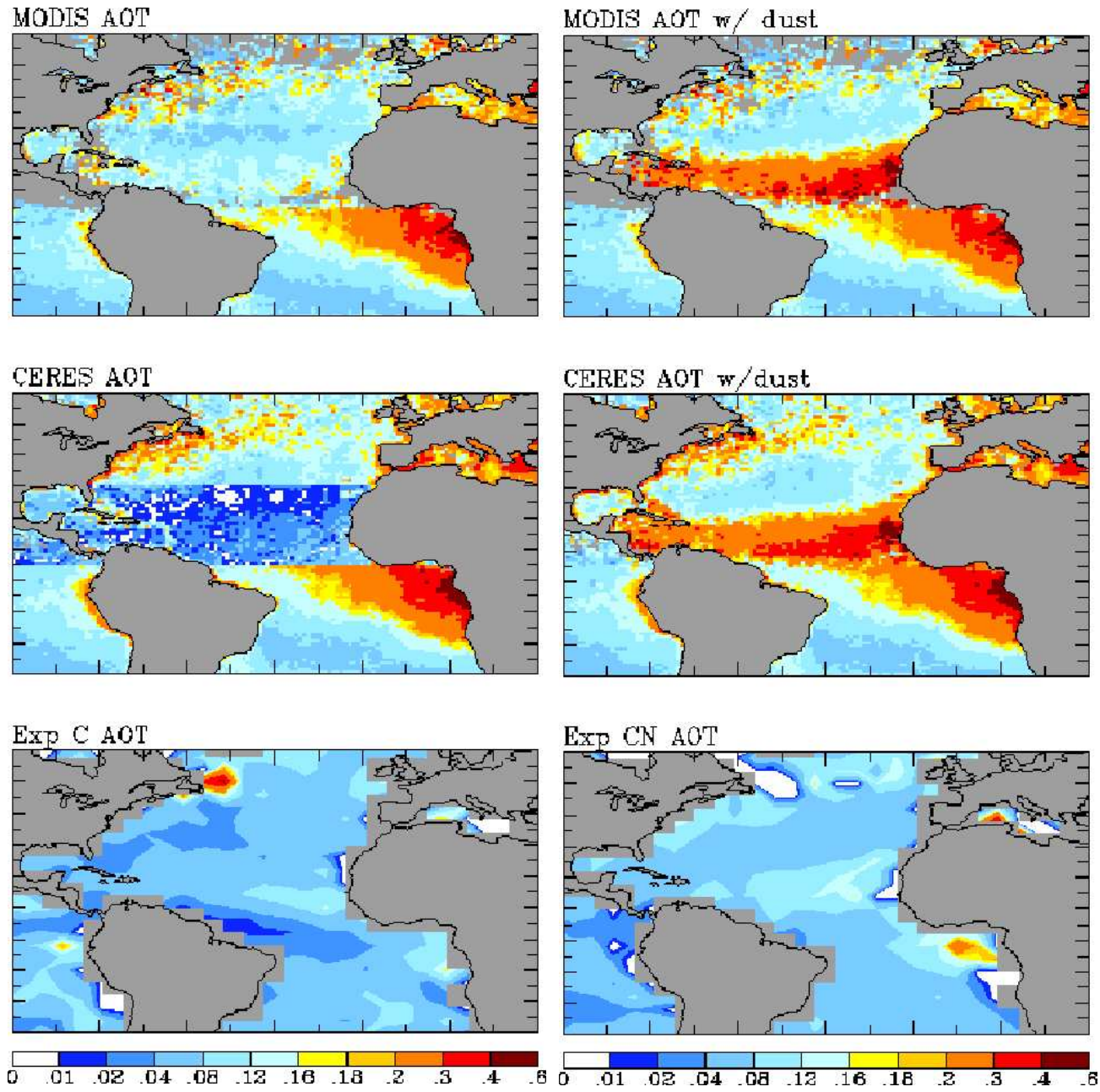

Figure 1. Aerosol optical thickness (AOT) for June-July-August (JJA) without and with the dust contribution to AOT from MODIS (top panel), CERES (middle panel), and AOT without the dust contribution as simulated by the model for Exp C and Exp CN (bottom panel).

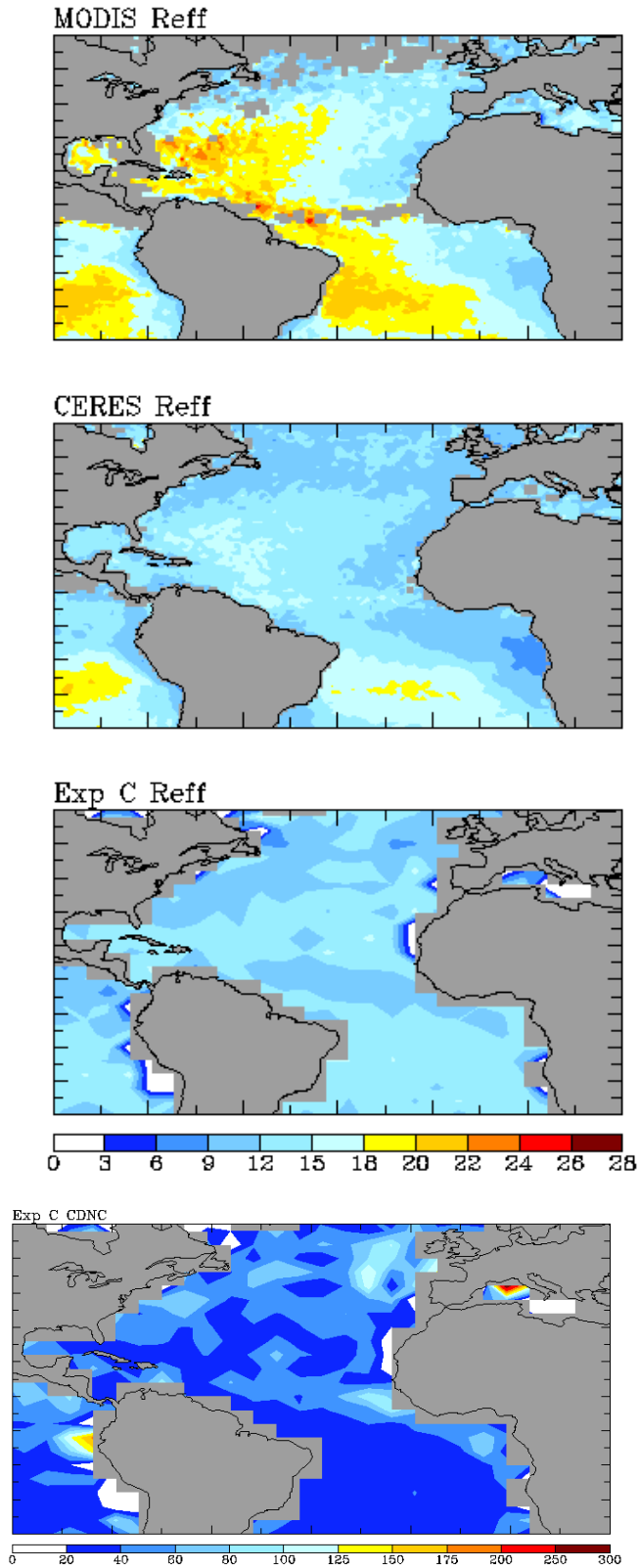

Figure 2. Cloud droplet effective radii (R_{eff}) (μm) for June-July-August (JJA) as retrieved from MODIS, CERES and as simulated by the model for Exp C. Also shown is the cloud droplet number concentration (CDNC) (cm^{-3}) for Exp C.

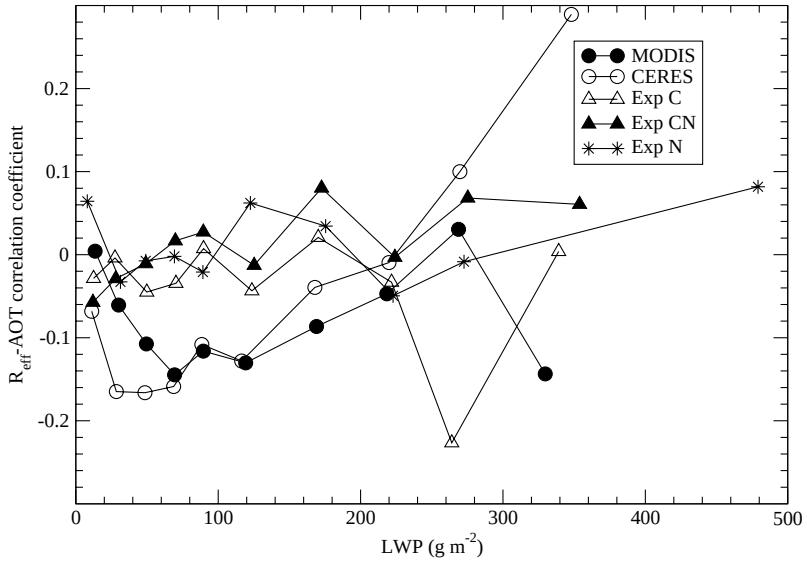

Figure 3. Correlation coefficients between cloud droplet effective radii (R_{eff}) and aerosol optical thickness (AOT) versus liquid water path (LWP) for June-July-August (JJA) as obtained from MODIS, CERES and as simulated by the model for Exp C, CN and N. Each point represents the average values over a given LWP range.

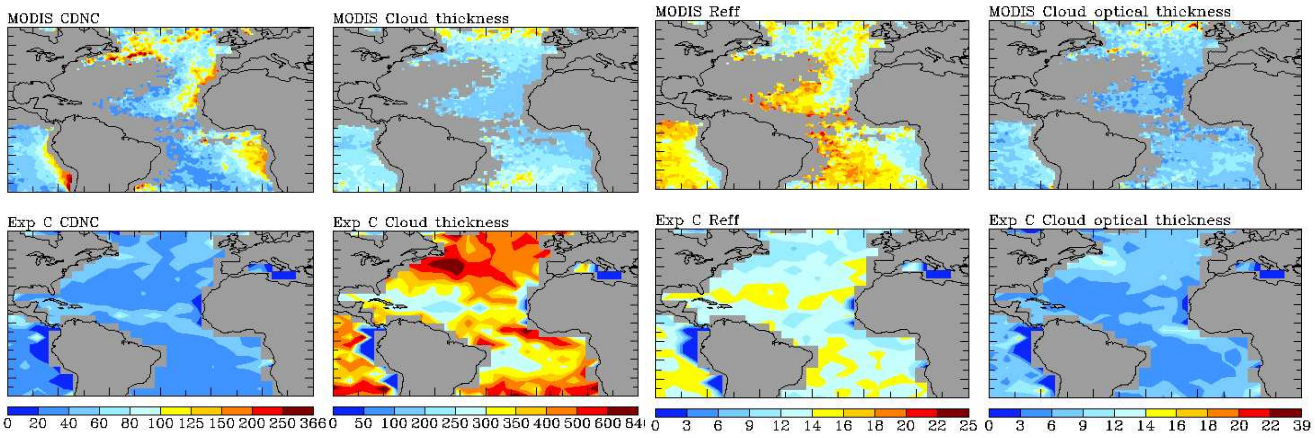

Figure 4. Cloud droplet number concentration (CDNC) (cm^{-3}), cloud thickness (m), cloud droplet effective radii (R_{eff}) (μm) and cloud optical thickness for June-July-August (JJA) as inferred from MODIS (onboard Aqua) and as simulated by the model for Exp C.

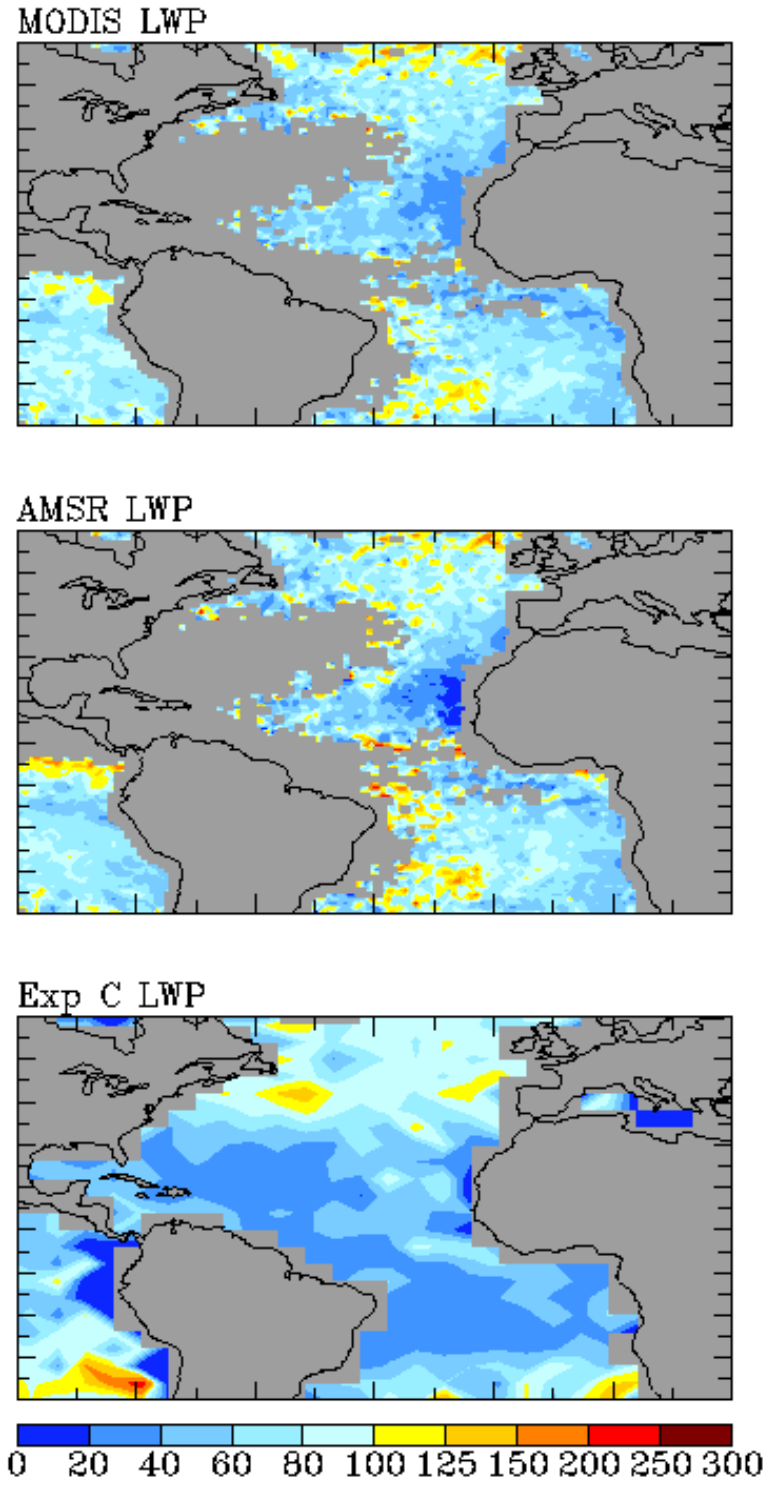

Figure 5. Liquid water path (LWP) (gm^{-2}) for June-July-August (JJA) as obtained from MODIS (onboard Aqua), AMSR-E and as simulated by the model for Exp C.

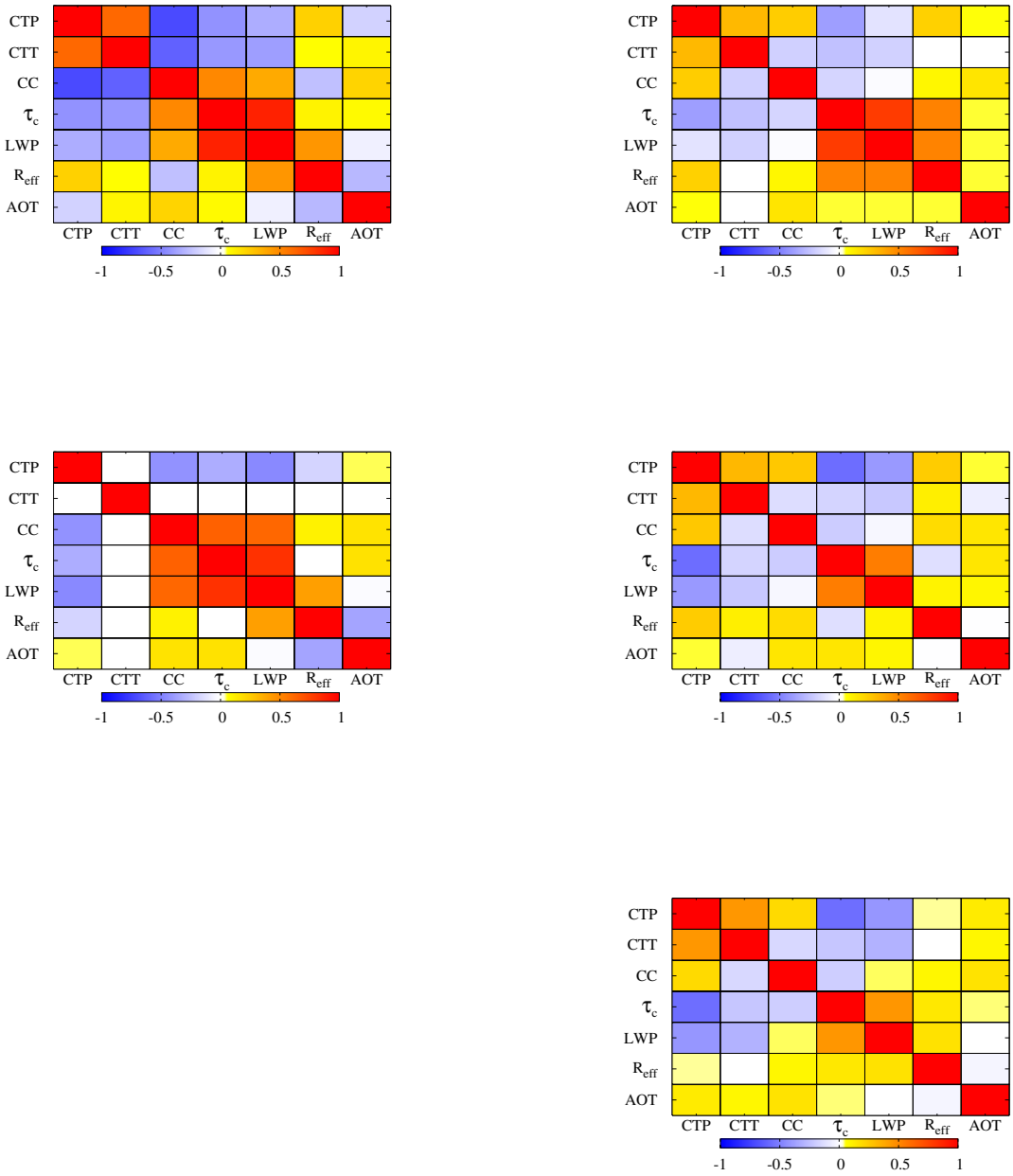

Figure 6. Correlation coefficients for the seven variables of interest for MODIS (top left), CERES (bottom left), Exp N (top right), Exp C (middle right) and Exp CN (bottom right). Values were significant at the 95% level for all data except for (1) Exp N: CTT-AOT, CTT-R_{eff}, (2) Exp C: R_{eff}-AOT, significant at the 90% level and (3) Exp CN: LWP-AOT, CTT-R_{eff}.

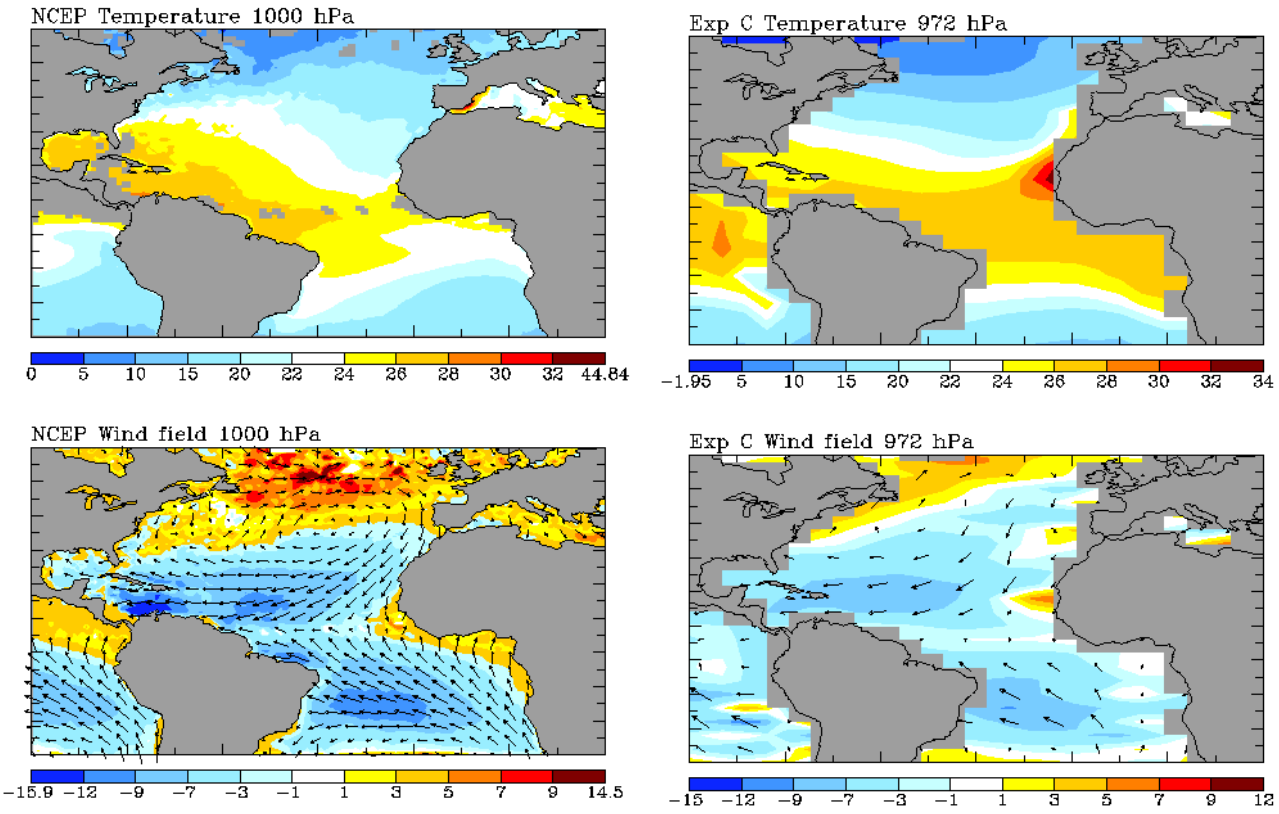

Figure 7. Temperature (C) and wind fields (ms^{-1}) from NCEP and Exp C for June-July-August (JJA).

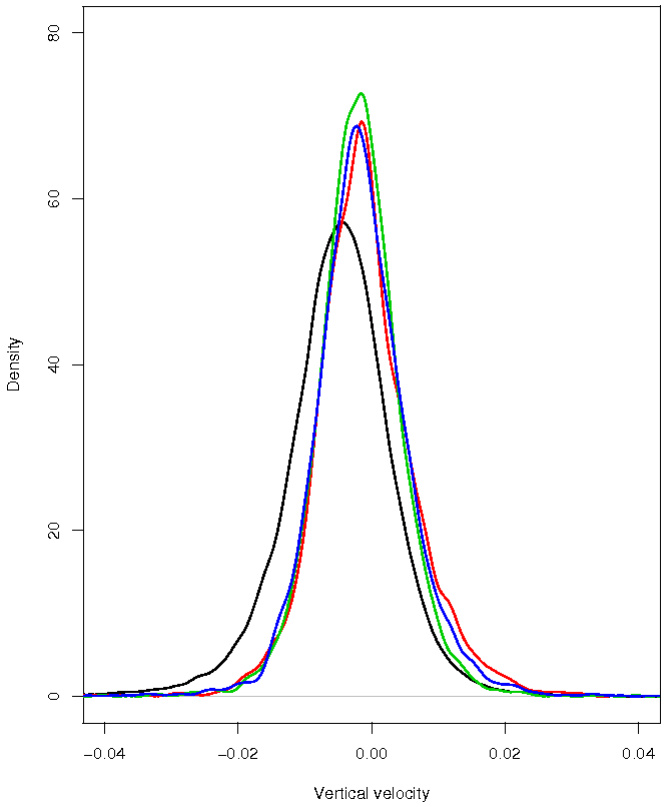

Figure 8. Probability density distribution of vertical velocity (ms^{-1}) at 750 hPa for June-July-August (JJA) as obtained from reanalysis data (NCEP) (black solid line) and as simulated by the model for all three simulations: Exp N (blue), Exp C (red) and Exp CN (green). Values are positive for upward direction.

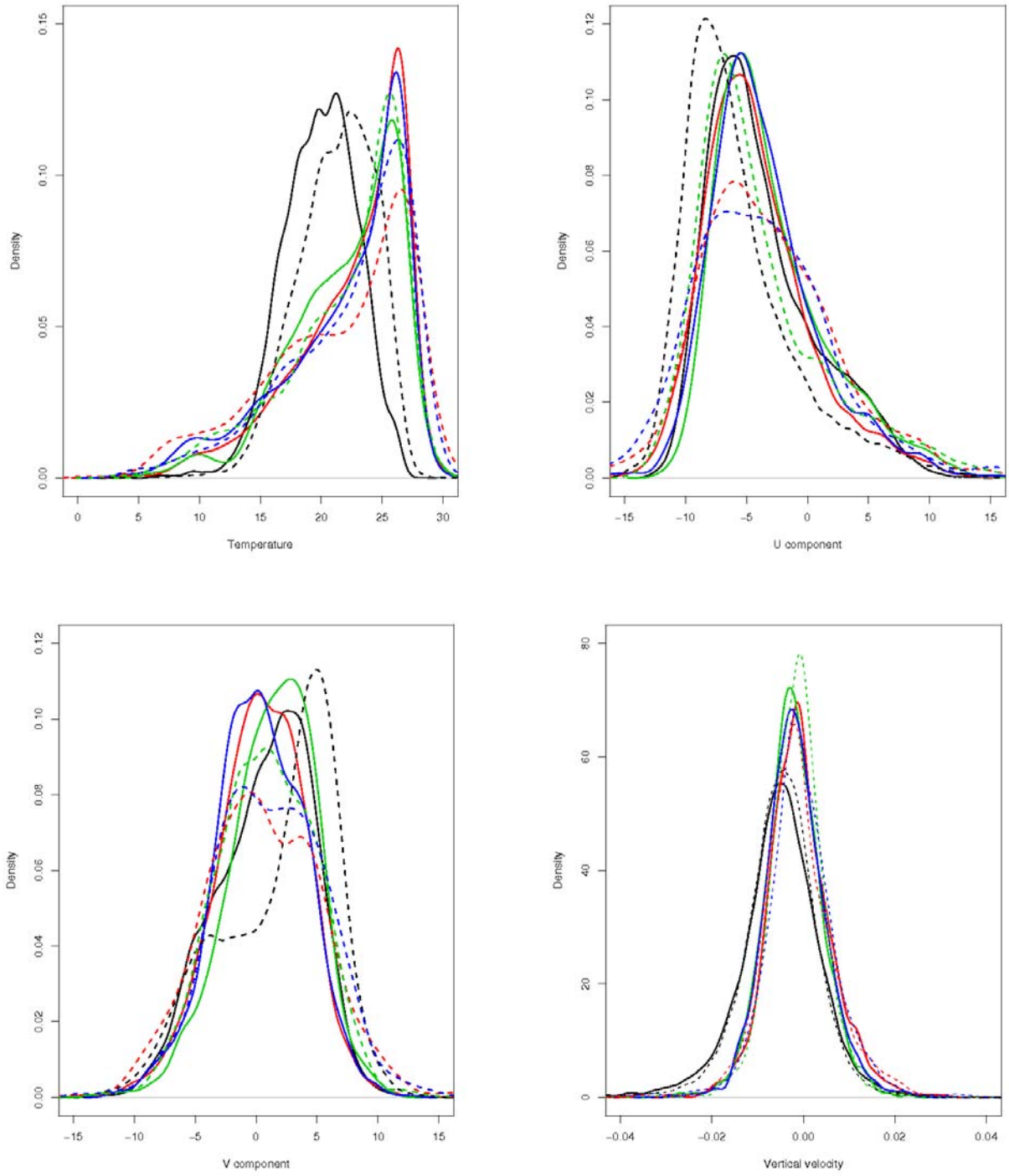

Figure 9. Probability density distributions for temperature (C), U and V components of winds (m/s) at 1000 hPa, and vertical velocities (m/s) at 750 hPa, for AOT <0.06 (solid) and AOT >0.06 (dashed) for NCEP (black), Exp N (blue), Exp C (red) and Exp CN (green) for June-July-August (JJA).